

Six Degree-of-Freedom Image Guidance for Frameless Intra-cranial Stereotactic RadioSurgery with kilo-voltage Cone-Beam CT

Zheng Chang^{1*}, Zhiheng Wang¹, Jinli Ma^{1,2}, Q. Jackie Wu¹, Ryan McMahon¹, John P. Kirkpatrick¹ and Fang-Fang Yin¹

¹Department of Radiation Oncology, Duke University Medical Center, Durham, NC, USA

²Department of Radiation Oncology, Fudan University Cancer Hospital, Shanghai, China

Abstract

Purpose: To investigate localization accuracy for frameless intracranial stereotactic-radiosurgery using 2D orthogonal planar imaging and 3D cone-beam CT (CBCT) in 6-degree-of-freedom (6-DOF).

Methods and Materials: In a phantom study, a target ball phantom was used to perform a Winston-Lutz test and to verify coincidence of imaging isocenter and radiation isocenter. A head phantom was placed with pre-defined positions and imaged with CBCT to test imaging accuracy. In a patient study, one hundred patients were included. Patients were initially positioned with a thermoplastic frameless mask system and then aligned with orthogonal planar imaging and CBCT. The setup discrepancies were quantitatively analyzed.

Results: Phantom experiments showed discrepancies in root-mean-square were 1.6mm translationally and 0.5° rotationally between CBCT 6-DOF image guidance and the known displacements after deviations from the radiation isocenter are considered. In the patient study, setup displacements between orthogonal planar imaging and CBCT 6-DOF image guidance were 3.2mm translationally and 0.9° rotationally. The positioning of twelve patients was corrected in 6-DOF using CBCT and a robotic couch to reduce translational and rotational discrepancies of 1.4mm and 1.3°, as compared with standard CBCT translational correction.

Conclusion: CBCT 6-DOF image guidance offers an explicit view to verify patient positioning in translations and rotations.

Keywords: Intra-cranial stereotactic radiosurgery; frameless; IGRT; 6-DOF; cone-beam CT

Introduction

Stereotactic radiosurgery (SRS) has been an effective treatment for the management of brain metastases and other brain diseases [1-6]. Traditionally, SRS is performed with the use of a stereotactic head ring frame. The head ring frame provides robust localization and minimal motion from CT-simulations to treatments [6-8]. However, the use of the conventional head ring often involves pain, general discomfort, and the need for surgical intervention. Recent developments in image-guidance and frameless immobilization enable target localization with increased accuracy, in order to deliver radiation more precisely to the tumor while sparing adjacent healthy tissue.

With the technical development, various frameless localization systems have been developed for stereotactic radiosurgery [8-20], as an alternative to the immobilization technology using the invasive head ring frame. Compared with the frame-based systems, these frameless systems offer better patient comfort, flexible treatment scheme, and the improved efficacy in utilization of resources. One such system is based on a customized bite-block made for an individual patient [9,10,12]. Similarly, another frameless system is based on a noninvasive thermoplastic mask system that is conformed to the patient's head [11]. Since the frameless mask systems are not always robust as the head ring frame, mechanic localizations used with the frameless mask systems may not necessarily warrant desirable location accuracy [18-20]. The frameless mask system shall always be used together with adequate image guidance for patient set-up and treatment localization. The accuracy of the localization is therefore dependent on the accuracy of the imaging guidance.

These imaging guidance systems can be either X-ray based or

Non-X-ray-based systems. The X-ray based systems includes, but not limited to, mega-voltage (MV) 2D electronic portal imaging devices (EPIDs), MV 3D fan-beam CT, kV on-board-imaging for 2D imaging and 3D cone-beam computed tomography (CBCT), in-room 3D CT scanners such as the CT-on-rails, the BrainLAB 6D ExacTrac system (BrainLAB, Heimstetten, Germany), and the Cyberknife kilo-voltage (KV) alignment system (Accuray, Inc., CA, USA). In addition to the X-ray image-based guidance systems, some other systems rely on other sources of information to position the patients for treatment, which includes AlignRT (Vision RT Inc., Boston, MA) for photogrammetry and the Calypso 4D Localization System (Calypso Medical Technologies, Inc., Seattle, WA) for electromagnetic tracking. Photogrammetry uses 3D surface imaging (either of the patient surface alone or with additional markers placed on the skin) for patient positioning. The Calypso 4D Localization System employs implanted electromagnetic transponders to track the position of the prostate.

In this work, our study focuses on the X-ray based systems, which can generally be grouped into two major categories: imaging guidance based on volumetric images and imaging guidance based

***Corresponding author:** Zheng Chang, Ph.D., Department of Radiation Oncology, Duke University Medical Center, Durham, NC 27710, USA, Tel: (919) 681-2608; Fax: (919) 681-7183; E-mail: zheng.chang@duke.edu

Received November 22, 2010; **Accepted** December 23, 2010; **Published** December 26, 2010

Citation: Chang Z, Wang Z, Ma J, Wu QJ, McMahon R, et al. (2010) Six Degree-of-Freedom Image Guidance for Frameless Intra-cranial Stereotactic RadioSurgery with kilo-voltage Cone-Beam CT. *J Nucl Med Radiat Ther* 1:101. doi:10.4172/2155-9619.1000101

Copyright: © 2010 Chang Z, et al. This is an open-access article distributed under the terms of the Creative Commons Attribution License, which permits unrestricted use, distribution, and reproduction in any medium, provided the original author and source are credited.

on planar images. The former category includes volumetric CBCT; the latter one involves on-board imager (OBI) orthogonal imaging. The key difference between the two imaging modalities is that CBCT imaging guidance is based on three-dimensional volumetric imaging matching while OBI orthogonal imaging based on two dimensional planar images. In three-dimensional CBCT images, anatomical structures and soft tissues are often better visualized than planar images. However, there are several concerns with the use of CBCT, including technical limitations, relatively long image acquisition time, and relatively high imaging dose to the patient. In contrast, OBI orthogonal imaging offers several benefits, including faster imaging time and less radiation to the patient. However, the 2D planar x-ray images may not always be optimal for image registration due to substantial overlapped structures. This is however completely resolved in CBCT since both treatment CBCT and planning CT offer high-quality volumetric images with clear details of both bony landmarks and soft tissues to use for high resolution registration. The volumetric high resolution registration makes 6-DOF image guidance more feasible to frameless intra-cranial SRS, particularly when mechanic localization is suboptimal.

In this work, we study localization accuracy for image-guided frameless intracranial SRS with a thermoplastic mask using KV 2D OBI orthogonal planar imaging and 3D CBCT. The feasibility of 6-degree-of-freedom (6-DOF) image-guidance using 3D CBCT is investigated.

Materials and Methods

Novalis Tx System with KV On-Board-Imager

The work was performed on a Novalis Tx system (Varian, CA, USA and BrainLAB, Heimstetten, Germany), which is equipped with the ExacTrac Robotics system (BrainLAB, Heimstetten, Germany) and the KV on-board-imager (OBI) with 2D and 3D KV imaging capabilities (Varian, CA, USA).

Exactrac robotics system: The exactrac robotics system, considered as a robotic couch, can be used for correcting patient position translationally and rotationally. The maximum compensation in pitch (lateral tilt) is $\pm 2.5^\circ$, while the maximum compensation in roll (longitudinal tilt) is $\pm 4^\circ$. When pitch reaches $\pm 2^\circ$, the maximum compensation in roll (longitudinal tilt) is limited $\pm 3^\circ$. The exactrac robotics system allows users to input manually desirable rotation parameters. Once the parameters are transferred into the system, the robotic couch is moved to reposition the patient and correct the setup error upon pressing the robotic enable bar of the control pendent.

Kv On-Board-Imager (Obi): The varian obi system consists of a kv x-ray source (kvs) and a kv amorphous silicon detector (kvd) with a sensitive area of $40 \times 30 \text{ cm}^2$, which are both mounted on the linear accelerator using robotic arms. The obi system provides three imaging modes: 2d radiographic acquisition, 2d fluoroscopic image acquisition, and 3d cone-beam computed tomography (cbct) acquisition. The 2d radiographic acquisition can be used to acquire 2d planar images at various angular positions at a selected source-to-imager distance. Generally, a pair of orthogonal images is taken to localize the target of interest. After the 2d radiographic acquisition is made, the acquired orthogonal planar images are aligned with the corresponding digital reconstructed radiographs (drr) in varian aria review software (version 8.6). The deviations are obtained to adjust positioning setup or for further analysis. The 3d cbct images are generated from 360 to 655 x-ray projections acquired over a certain range of gantry rotation. There are six cbct models available in

the system: low-dose head, standard-dose head, high-quality head, pelvis spotlight, pelvis, and low-dose thorax. The first four modes are scanned with "full-fan" acquisition, where 360 projections are acquired over a gantry rotation of 200 degrees, while the last two modes are scanned with "half-fan" acquisition where 655 projections are acquired over a complete gantry rotation. The slice thickness can be selected from 2.5 mm up to 1.0 mm for each mode. Given the difference of various modes, the cbct mode should be selected to reach the optimal balance between image quality, image time and image dose for each patient. Generally, the full-fan acquisition is used to image small diameter anatomic sites such as brain, while the half-fan acquisition for large diameter anatomic sites such as pelvis and chest. In this work, the full-fan high-quality head acquisition is selected for the study. After cbct acquisition is made, the corresponding planning ct and anatomic structure contours are aligned with the cbct images in varian aria review software to adjust positioning setup or for further analysis.

Setup measurements

Winston-Lutz Test with Verification of Accuracy of OBI imaging system: Due to the tight margins of stereotactic radiosurgery treatments, the mechanical and radiation isocenter of the linear accelerator should be verified, typically using a Winston-Lutz test [2,6]. The setup for a Winston-Lutz test is illustrated in Figure 1, where the simulated target ball is placed at the radiation isocenter and the gantry/couch are rotated in different combinations as the ball is imaged using films (e.g. radiochromic films). Accuracy should be kept to within 1mm [2,6].

After the Winston-Lutz test is passed, the accuracy of OBI imaging system is verified with simulated target ball placed at the radiation isocenter. More specifically, two orthogonal planar images are taken respectively at anterior-posterior (AP) and right-lateral (RLAT) positions at the source to imager distance of 150cm. The radiologic settings are: peak voltage (kVp): 100, tube current (mA): 200, exposure time (ms): 40 for AP imaging; kVp: 100, mA: 200, ms: 40 for RLAT imaging, which are standard radiologic settings for head KV planar imaging. After this, a volumetric CBCT scan was acquired in full-fan high quality head mode (FOV = 25cm; Matrix = 384×384 ; axial dimensional coverage = 17cm; slice thickness = 1.0 mm). The center of the simulated target ball is considered as the radiation isocenter, and as such the deviations of OBI imaging isocenter center from the radiation isocenter are obtained using the KV planar images and CBCT. The deviations of the build-in cross-hair in the treatment head from the radiation isocenter can also be obtained, which will be used for the following phantom study. The above procedure was repeated for five times.



Figure 1: The setup from two different views for a Winston-Lutz test with the simulated target ball at the isocenter.

Head phantom study: Prior to enrollment of patients, a head phantom study was carried out using a CIRS (computerized Imaging Reference Systems, Inc., Norfolk, VA) model 605 radiosurgery anthropomorphic head phantom. The anthropomorphic phantom contained bone and soft tissue with attenuation characteristics that simulated a human head. As a result, transmission and tomographic images of the phantom appeared similar to patient anatomy on KV X-ray imaging systems.

The phantom was scanned in helical mode on a GE multislice CT scanner (Lightspeed, General Electric Medical Systems, Waukesha, WI) with a clinical head protocol (FOV = 40 cm; Matrix = 512x512; slice thickness = 1.25mm). After the completion of the scan, the CT images were exported to Varian Eclipse treatment planning systems. In Eclipse treatment planning system, a planning target volume (PTV) was manually contoured to simulate a centrally located brain lesion. A treatment plan was then developed with a single static beam with isocenter located at approximately the center of PTV. Finally, the plan was approved in Varian Eclipse and the corresponding CBCT setup was generated for the phantom study.

The phantom was initially positioned on the couch using the marks on the surface of the head phantom and the build-in cross-hair in the treatment head. A known 6D shift including pitch, roll, and yaw was performed. More specifically, translational shift was selected from (0.00, -10.00, -20.00, 10.00, 20.00 mm), while rotational shift was selected from (0.00, -1.50, -0.50, 1.50, 0.50) [21]. The phantom was then imaged with both 2D radiographic mode and 3D CBCT as described in the previous section. The acquired orthogonal planar images are matched manually with the corresponding DRRs, while the CBCT images were matched with the planning CT. The discrepancies between acquired images with planning images can be considered as deviations of "ideal" positioning setup from imaging isocenter and coordinate system. By including the previously measured deviations of the build-in cross-hair from the radiation isocenter, the discrepancies through the imaging matching could be used to derive the deviations of imaging localization from the radiation isocenter. In other words, the comparison of measured versus known displacements added with measured deviations of the build-in cross-hair from the radiation isocenter was used to test the accuracy of image guidance for correcting translational and rotational setup errors. The phantom test was repeated for five times.

Patient Study: In this work, one hundred intracranial SRS patients were randomly selected for a retrospective analysis. Each patient received a single-fractional SRS treatment with a dose ranging from 12Gy to 24Gy. Patients were positioned supine on the couch in a neutral position and immobilized with a BrainLAB thermoplastic head mask system (BrainLab, Heimstetten, Germany). The system consists of U-shape metal frame, a customized mask conformed to the patient, three reinforcing straps and an intraoral thermoplastic piece. To enhance the immobilization, the three thermoplastic reinforcing straps were used under the mask over the forehead, below the nose, and over the chin. Furthermore, the intraoral piece was positioned in the mouth against the upper dentition to minimize a possible head tilt. All the patients were scanned on a GE multislice CT scanner (Lightspeed, General Electric Medical Systems, Waukesha, WI) with a clinical head protocol (FOV = 40 cm; Matrix = 512x512; slice thickness = 1.25mm). Structure contouring and treatment planning were performed and approved in the BrainLAB iPlan treatment planning system (BrainLab, Heimstetten, Germany). After that, all the structures, CT images and treatment plans were exported to Varian Eclipse system. All treatment plans were delivered at the Novalis Tx system.

Patients were initially positioned with the BrainLAB frameless mask system with target-positioning-overlays (TAPO). Two orthogonal 2D KV images were then taken to verify the patient's initial setup with the same radiographic setting as the phantom study. After this, the patients were scanned using CBCT in a full-fan High-Quality Head mode with a slice thickness of 1.0 mm. The CBCT images could be registered with the corresponding planning CT images using Varian Aria review software in three translational directions and one rotational direction (yaw), in 4 degree-of-freedom (4-DOF). The CBCT images could also be fused with the planning CT images in 6 degree-of-freedom (6-DOF). If necessary, the 6-DOF positioning discrepancies can be corrected by using the robotic couch. Treatment delivery began after the CBCT image match was confirmed.

Generally, the 6-DOF position correction may take more efforts and time than a standard translational setup correction. To optimize the efforts and performance, the following criteria are generally followed at our institute to determine whether a 6-DOF position correction shall be made: (1) rotational error is greater than 1 degree; (2) tumor shape is irregular; and (3) tumor is close to critical organs such as brainstem.

Statistical analysis

In this study, all the translational and rotational displacements were illustrated according to the International Electrotechnical Commission (IEC) coordinates to facilitate quantitative analysis. More specifically, according to IEC coordinates, the positive directions of coordinates X, Y, Z correspond to the left, superior, and anterior anatomic directions, respectively, if a patient is positioned supine with head toward the gantry. Pitch, roll, and yaw correspond to the rotations around the X (i.e., left-right, [LR]), Y (i.e., superior-inferior, [SI]), and Z (i.e., anterior-posterior, [AP]) axes, respectively. In this work, the setup discrepancies were calculated and quantified using the root-mean-square (RMS) and standard deviation (SD). The overall translational and rotational discrepancies in RMS can be calculated as follows:

$$TD = \sqrt{LR^2 + SI^2 + AP^2} \quad (1)$$

$$RD = \sqrt{Pitch^2 + Roll^2 + Yaw^2} \quad (2)$$

where *TD* and *RD* are referred as overall translational and rotational discrepancies, respectively.

The paired Student's t-test was used to test the setup differences, and to evaluate the changes in setup differences caused by CBCT 3D image fusion and CBCT 6D image fusion. Statistical significance was considered at $p < 0.05$.

Results

Measurements for Winston-Lutz Test and Verification of Accuracy of OBI imaging system

Figure 2 shows a representative example of a passed Winston-Lutz test film, in which outer sphere was generated by a 7.5 mm-diameter cone and inner sphere is created by 5mm-diameter target ball placed at the radiation isocenter. Considerable margins between inner and outer spheres indicated the deviation of mechanical and radiation isocenter of the linear accelerator is less than 1.0 mm [2,6]. Figure 3 shows a representative example of OBI orthogonal images of a simulated ball target right after a passed Winston-Lutz test. The discrepancies in RMS are 0.67 mm in LR, 0.92 mm in SI, and 0.65 mm in AP, with a TD value of 1.31 mm. The corresponding standard

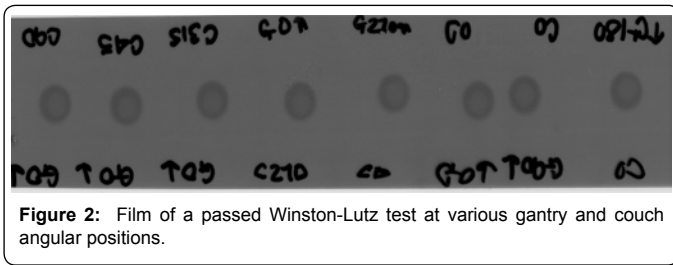


Figure 2: Film of a passed Winston-Lutz test at various gantry and couch angular positions.

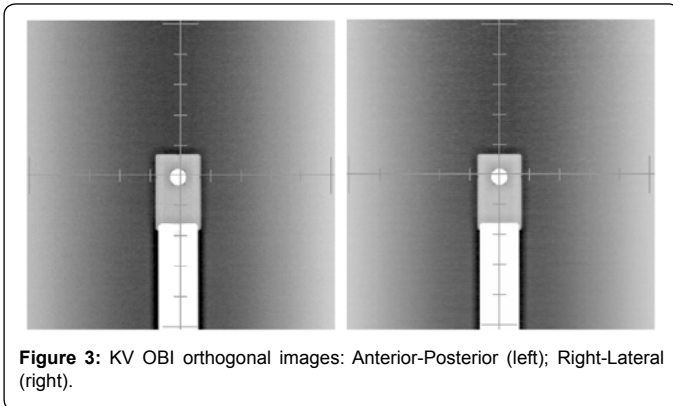


Figure 3: KV OBI orthogonal images: Anterior-Posterior (left); Right-Lateral (right).

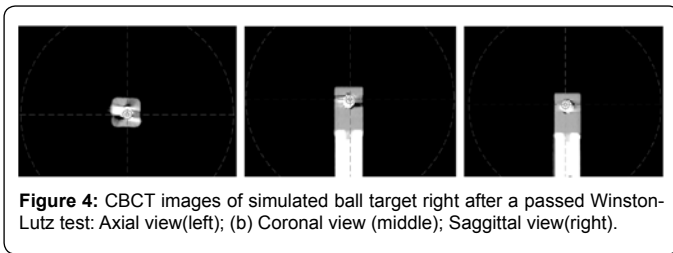


Figure 4: CBCT images of simulated ball target right after a passed Winston-Lutz test: Axial view(left); (b) Coronal view (middle); Saggittal view(right).

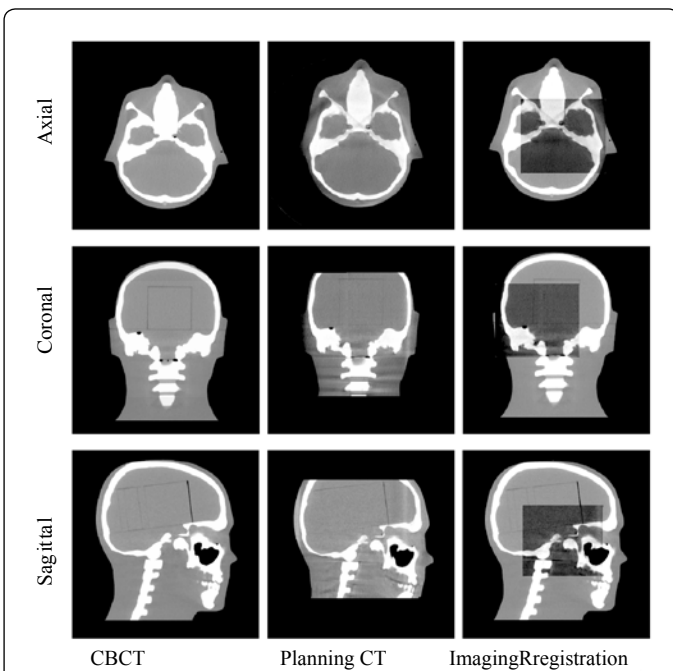


Figure 5: Representative example of a head phantom's CBCT image registrations: planning CT, cone-beam computed tomography (CBCT), and matched images.

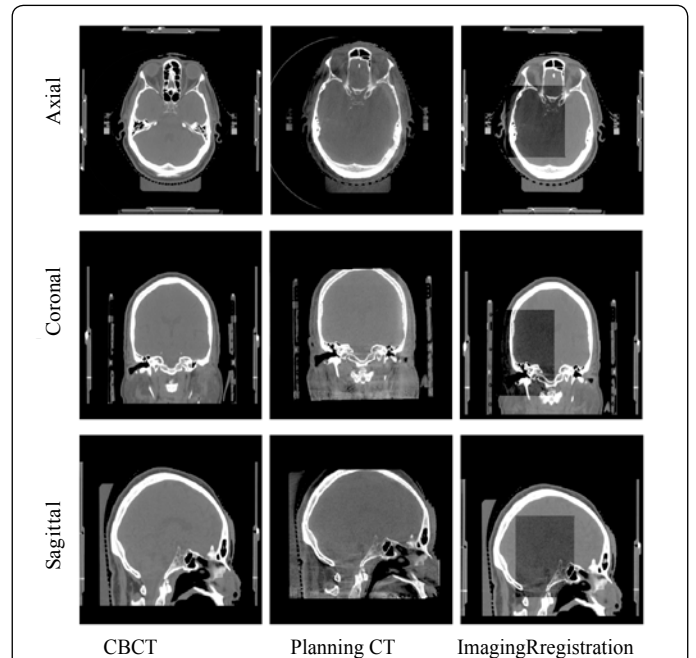


Figure 6: Representative example of a patient's image registrations: (a) planning CT, cone-beam computed tomography (CBCT), and matched images.

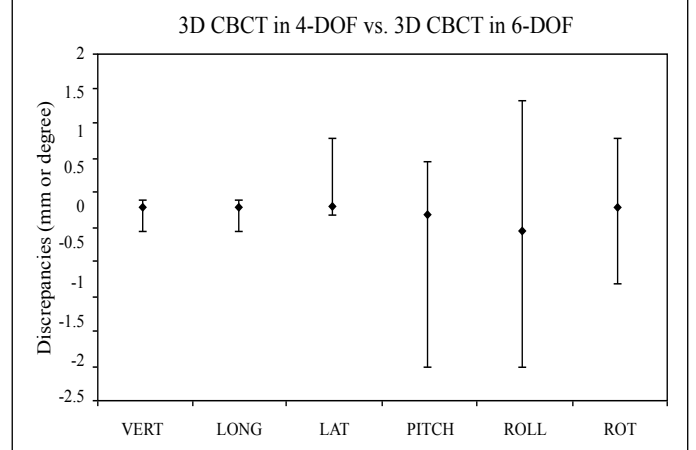
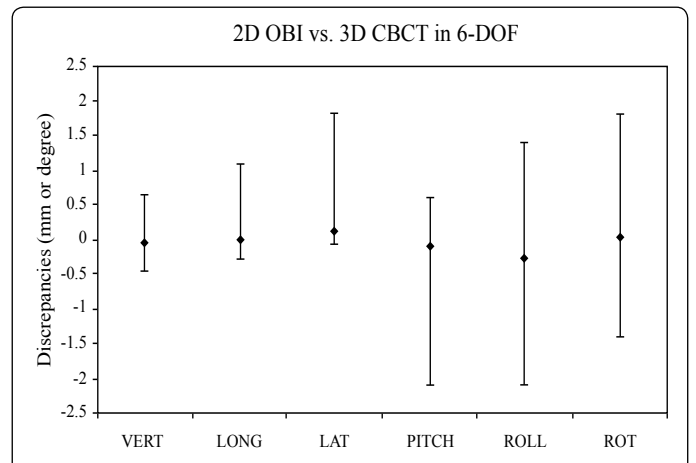
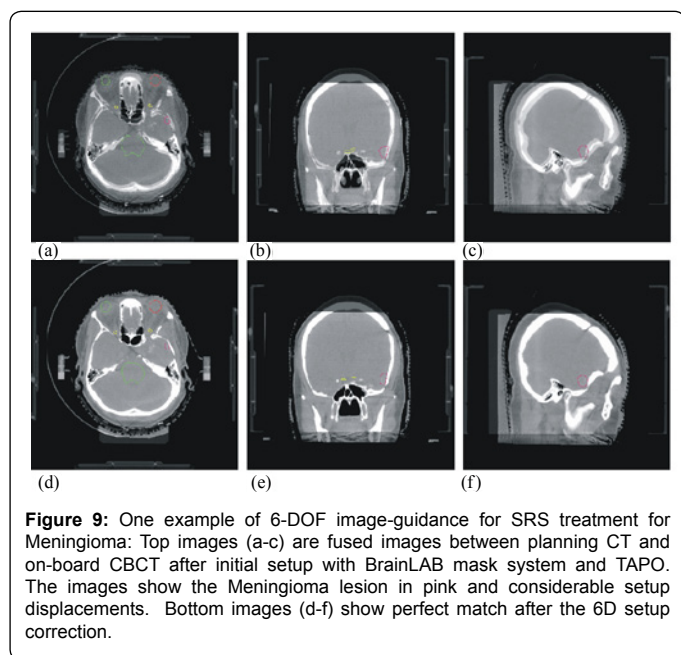
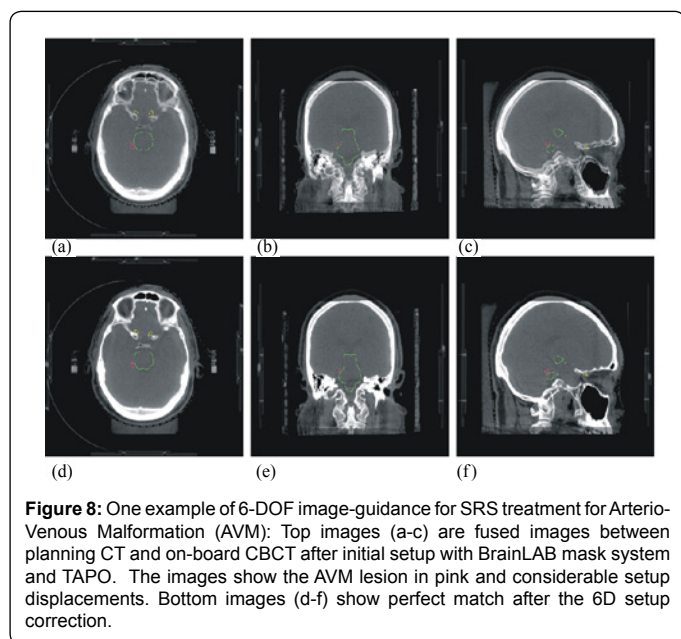


Figure 7: Patient Study: setup discrepancies in millimeters and degrees for 2D OBI, 3D CBCT match in 4-DOF and 3D CBCT match in 6-DOF in the three orthogonal directions (AP, SI and LR) and in three rotations (pitch, roll and yaw).



deviations are 0.13 mm in LR, 0.19 mm in SI, and 0.22 mm in AP. Figure 4 shows a representative example of CBCT images of the simulated ball target right after the passed Winston-Lutz test. The discrepancies in RMS are 0.89 mm in LR, 1.16 mm in SI, and 0.60 mm in AP, with a TD value of 1.58 mm. The corresponding standard deviations are 0.24 mm in LR, 0.11 mm in SI, and 0.13 mm in AP. The discrepancies in RMS between OBI orthogonal imaging and CBCT are 0.35 mm in LR, 0.36 mm in SI, and 0.19 mm in AP, with a TD value of 0.53 mm. The corresponding standard deviations are 0.29 mm in LR, 0.28 mm in SI, and 0.19 mm in AP. The measurements demonstrated that the imaging isocenters of the orthogonal imaging and CBCT are generally consistent.

Setup measurements for phantom study

Figure 5 shows a representative example of a phantom planning

CT image and CBCT images. The phantom experiments showed that the RMS of the discrepancies in translations and rotations were less than 1.2 mm for each direction and 0.5° for each rotation between CBCT 6D image fusion and the known setup displacements, after the deviations from the radiation isocenter is taken into account. More specifically, the corresponding rotational setup discrepancies in RMS were 0.38° in pitch, 0.19° in roll, and 0.22° in yaw. The translational discrepancies in RMS were 0.95 mm in LR, 1.01 mm in SI, and 0.86 mm in AP. The overall discrepancies from the radiation isocenter in translations and rotations were $TD = 1.63$ mm and $RD = 0.48^\circ$. The measured data were also summarized in Table 1. The phantom data show consistent measurements as those measured using CBCT images of the simulated ball target right after the passed Winston-Lutz tests. The consistency suggests that the CBCT imaging of a simulated ball target right after a passed Winston-Lutz test can be used adequately to verify the accuracy of CBCT isocenter periodically, due to its efficiency and convenience.

Setup measurements for patient study

The setup discrepancies between OBI orthogonal images and CBCT were retrospectively measured for one hundred patient cases. Figure 6 shows a representative example of a patient's planning CT, CBCT images, and fused images, as seen during one session of image registration. The RMS and SD of the setup discrepancies were calculated for all patients. The differences between initial setup with TAPO and CBCT 6D image fusion were found to be considerable. As illustrated in Table 2, the differences in RMS between initial setup with TAPO and CBCT 6-DOF image guidance was greater than 1.5 mm in all the three translational directions. The corresponding rotational discrepancies in RMS between initial setup with TAPO and CBCT image guidance in 6-DOF was 0.45° in pitch, 0.62° in roll, and 0.59° in yaw, respectively. The overall discrepancies in translations and rotations were $TD = 3.6$ mm and $RD = 1.0$.

The RMS and SD of the setup discrepancies between 2D OBI match and CBCT in 6-DOF were calculated, as shown in Table 2. The overall discrepancies between the two imaging modalities in translations and rotations were $TD = 3.2$ mm and $RD = 0.92^\circ$. Similarly, the RMS and SD of the setup discrepancies between CBCT match in 4-DOF and CBCT in 6-DOF were also calculated, as illustrated in Table 3. In general, the RMS of the differences was < 1.0 mm translationally and < 1.0° rotationally for each direction. The overall discrepancies were $TD = 1.3$ mm and $RD = 0.8^\circ$, much less than those by TAPO and OBI. The differences were, however, found to be statistically significant in the translation of LAT ($p = 0.041$). The setup differences are illustrated in Figure 7 for easy comparison.

CBCT imaging match in 6-DOF was used to evaluate the positioning of all the 100 patients. Six degree-of-freedom setup correction was applied to twelve patients using the robotic couch. After the 6-DOF setup correction, the translational and rotational positioning discrepancies in RMS were effectively reduced by 1.4 mm and 1.3°, as compared to standard translational setup correction. Two representative cases are illustrated in Figures 8 and 9.

Discussions

In this work, both phantom and patient measurements were acquired, which showed the effectiveness of CBCT image guidance to minimize setup errors in 6-DOF including pitch and roll. The overall discrepancies of CBCT image guidance were found in the ball target phantom and the anthropomorphic head phantom to be < 1.8 mm in translations and < 0.5° in rotations, after the deviations from

Displacement direction		Discrepancies between CBCT 6-DOF match and known displacements including deviations from the radiation isocenter (RMS, SD)
Translation (mm)	AP	0.86, 0.49
	SI	1.01, 0.30
	LR	0.95, 0.33
Rotation (degree)	Pitch	0.38, 0.37
	Roll	0.19, 0.10
	Yaw	0.22, 0.19

Table 1: Translational and rotational discrepancies between CBCT 6D image registration and known displacements in a head phantom study. Abbreviations: LR = left-right; SI = superior-inferior; AP = anterior-posterior; Pitch = rotation around LR direction; Roll = rotation around SI direction; Yaw = rotation around AP direction.

Displacement direction		Discrepancies by OBI (RMS, SD)	Discrepancies by CBCT in 4-DOF (RMS, SD)	Discrepancies by CBCT in 6-DOF (RMS, SD)	OBI vs. CBCT in 6-DOF Difference (RMS, SD)		CBCT in 4-DOF vs. CBCT in 6-DOF Difference (RMS, SD)	
						p-value		p-value
Translation	AP	1.19, 0.89	1.69, 1.22	1.90, 1.33	1.33, 1.25	<0.01	0.63, 0.63	0.208
	SI	2.07, 1.56	2.09, 1.63	2.34, 1.69	1.65, 1.66	0.857	0.54, 0.54	0.068
	LR	1.01, 0.86	1.91, 1.85	1.90, 1.84	2.38, 2.09	<0.01	0.98, 0.97	0.041
Rotation	Pitch	0.0, 0.0	0.0, 0.0	0.45, 0.44	0.45, 0.44	0.026	0.62, 0.56	0.026
	Roll	0.0, 0.0	0.0, 0.0	0.62, 0.56	0.62, 0.56	<0.01	0.62, 0.56	<0.01
	Yaw	0.05, 0.32	0.71, 0.70	0.59, 0.59	0.53, 0.53	0.835	0.39, 0.39	0.098

Table 2: Translational and rotational displacements according to CBCT in patient studies.

Study (reference)	Immobilization device	Imaging modality	Mean ± SD for positioning errors (mm)
Baumert et al. 2005 (22)	Thermoplastic mask alone	CT	3.7 ± 2.8
	Thermoplastic mask with bite block		2.2 ± 1.1
	Thermoplastic mask with upper jaw support		3.3 ± 1.8
Boda-Heggemann et al. 2006 (20)	Scotch-cast rigid mask	kv-CBCT (Elekta)	3.1 ± 1.5
	Thermoplastic mask		4.7 ± 1.7
Guckerberger et al. 2007 (21)	Scotch-cast rigid mask	kv-CBCT (Elekta)	3.0 ± 1.7
Masi et al. 2008 (18)	Thermoplastic mask alone	kv-CBCT (Elekta)	3.0 ± 1.4
	Thermoplastic mask with bite block		2.9 ± 1.3
Present study	U-frame mask with bite block	kv-CBCT (Varian)	3.6, 1.9*

*RMS and SD for translations in all three directions

Table 3: Positioning errors in cranial noninvasive frameless systems measured with CT/CBCT.

the radiation isocenter is taken into account. In the retrospective patient studies, there are considerable setup displacements between 2D OBI image match and CBCT image match in 6-DOF: $TD = 3.2\text{mm}$ translationally and $RD = 0.9^\circ$ rotationally. If positioning was corrected in 4-DOF with CBCT, the residual translational and rotational discrepancies were $TD = 1.3\text{ mm}$ and $RD = 0.8^\circ$, as compared with CBCT image match in 6-DOF.

In this work, the accuracy of OBI orthogonal imaging and CBCT was verified by using a simulated ball target through a standard Winston-Lutz test. The data of the ball target phantom show a TD value of 0.53 mm for the discrepancies between OBI orthogonal imaging and CBCT, which demonstrate consistent accuracy for the two imaging guidance modalities. However, the larger discrepancies between the two imaging modalities of the patient data suggest that patients' rotation may be a potential source of such discrepancies in a frameless localization system. As indicated by the ball target measurements, the standard deviations showed much less in value than the discrepancies in RMS between the imaging isocenter and the radiation isocenter. Generally, the less standard deviation is, the less random error. The results suggest that the accuracy of the OBI imaging system can be potentially improved by using the radiation isocenter as the calibration benchmark.

Although this work showed 6-DOF imaging guidance using CBCT, there are other imaging guidance systems offering 6-DOF image guidance. One alternative technique is ExacTrac X-Ray 6D (BrainLAB, Heimstetten, Germany), in which two oblique high-quality radiographs are acquired. After a pair of radiographic images is acquired, the KV images are fused with the DRRs obtained from simulation CT images using either 3-DOF or 6-DOF imaging fusion algorithms. The radiographs are two dimensional projections along two oblique angles, and as such substantial overlapped structures may appear in the 2D radiographic images. It has been reported that there are considerable localization discrepancies between ExacTrac X-Ray 6D and CBCT [17, 21]. Given the fact that the radiographs are taken obliquely rather than standard orthogonal settings,

intervention by users is challenging, particularly when visible spatial discrepancies appear due to undesirable rotations. The weakness may be partially compensated by several benefits offered by ExacTrac X-Ray 6D, including faster and automatic setup, motion tracking, and less radiation to the patient.

The study demonstrated minor discrepancies between CBCT 4-DOF image guidance and CBCT 6-DOF image guidance. The overall translational discrepancies are generally less than 1.3 mm; the overall rotational discrepancies are within 0.8° . The discrepancies shall not be ignored. First, in certain cases, tumor is in an irregular shape and close to critical organs. Rotational discrepancies may compromise the adequate dose coverage for the target while delivering overdose to critical organ. One example is illustrated in Figure 8, where tumor is elongated and right besides brainstem. Second, the translational discrepancies may potentially be caused by the uncorrected rotational errors, particular in roll, in CBCT 4-DOF image guidance. Over 35 patients of the 100 cases, translational discrepancies show 1.0 mm or greater along one translational direction if 6-DOF positioning correction was not used, which may be clinically considerable in SRS. This implies that uncorrected rotational errors can introduce unintentional translational errors, which are demonstrated in the study.

In the study, overall setup displacements between mechanic TAPO setup and CBCT 6D image fusion were found to be 3.6mm translationally and 1.0° rotationally when thermoplastic mask-based relocatable immobilization systems were used. This finding is consistent with data reported by other works published in literature [16,18,20]. This implies that adequate imaging guidance shall be used together with mask-based relocatable immobilization systems to ensure the precise localization of targets. When independent imaging systems are available, it is recommended to verify patient position using a second localization system.

In this work, CBCT 6-DOF image guidance was employed to verify patient positioning in both translations and rotations, making full use

of 3D CBCT data. The phantom study showed that CBCT 6-DOF image guidance was an acceptable image-guided localization technique for frameless SRS. In our clinic, CBCT 6-DOF image fusion has been often used with the robotic couch to correct translational and rotational setup errors for SBRT, SRS and SRT treatments, minimizing setup errors.

Conclusions

Due to relatively large setup displacements, frameless thermoplastic mask system with TAPO should only be used for stereotactic radiosurgery with accurate imaging guidance. CBCT 6-DOF image guidance offers explicit view to verify patient positioning in both translations and rotations. Combined with a robotic couch, translational and rotational setup errors can be effectively minimized. Although the CBCT 6-DOF image fusion with a robotic couch was demonstrated with only intra-cranial cases in this work, the principle can be extended to extra-cranial stereotactic radiosurgery for improved patient positioning accuracy.

Acknowledgement

Authors would like to thank Ms. Robyn Walker, Ms. Breann Bollinger, RTT, Ms. Charlotte Deakin, RTT, and Ms. Samantha Allen, RTT for their assistance with data acquisition.

References

1. Leksell L (1951) The stereotaxic method and radiosurgery of the brain. *Acta Chir Scand* 102: 316-319.
2. Lutz W, Winston KR, Maleki N (1988) A system for stereotactic radiosurgery with a linear accelerator. *Int J Radiat Oncol Biol Phys* 14: 373-381.
3. Kondziolka D, Patel A, Lunsford LD, Kassam A, Flickinger JC (1999) Stereotactic radiosurgery plus whole brain radiotherapy versus radiotherapy alone for patients with multiple brain metastases. *Int J Radiat Oncol Biol Phys* 45: 427-434.
4. Sneed PK, Suh JH, Goetsch SJ, Sanghavi SN, Chappell R, et al. (2002) A multi-institutional review of radiosurgery alone vs. radiosurgery with whole brain radiotherapy as the initial management of brain metastases. *Int J Radiat Oncol Biol Phys* 53: 519-526.
5. Aoyama H, Shirato H, Tago M, Nakagawa K, Toyoda T, et al. (2006) Stereotactic radiosurgery plus whole-brain radiation therapy vs stereotactic radiosurgery alone for treatment of brain metastases: a randomized controlled trial. *JAMA* 295: 2483-2491.
6. Schell M, Bova F J, Larson D, Leavitt D, Lutz W , et al. (1995) Stereotactic radiosurgery Report of AAPM TG 42.
7. Yeung D, Palta J, Fontanesi J, Kun L (1994) Systematic analysis of errors in target localization and treatment delivery in stereotactic radiosurgery (SRS). *Int J Radiat Oncol Biol Phys* 28: 493-498.
8. Kitchen ND, Lemieux L, Thomas DGT (1993) Accuracy in frame-based and frameless stereotaxy. *Stereotact Funct Neurosurg* 61: 195-206.
9. Bova FJ, Meeks SL, Friedman WA, Buatti JM (1998) Optic-guided stereotactic radiotherapy. *Med Dosim* 23: 221-228.
10. Meeks SL, Bova FJ, Wagner TH, Buatti JM, Friedman WA, et al. (2000) Image localization for frameless stereotactic radiotherapy. *Int J Radiat Oncol Biol Phys* 46: 1291-1299.
11. Breneman JC, Steinmetz R, Smith A, Lamba M, Warnick RE (2009) Frameless image-guided intracranial stereotactic radiosurgery: clinical outcomes for brain metastases. *Int J Radiat Oncol Biol Phys* 74: 702-706.
12. Furuse M, Aoki T, Takagi T, Takahashi JA, Ishikawa M (2008) Frameless stereotactic radiosurgery with a bite-plate: our experience with brain metastases. *Minim Invasive Neurosurg* 51: 333-335.
13. Chang J, Yenice KM, Narayana A, Gutin PH (2007) Accuracy and feasibility of cone-beam computed tomography for stereotactic radiosurgery setup. *Med Phys* 34: 2077-2084.
14. Wang Z, Kirkpatrick J, Wu Q, Chang Z, Willett C, et al. (2009) Comparison of Cone-Beam CT and Frame-Based Localizations for Stereotactic Radiosurgery with Fixed Head Rings and Removable Frames. *Medical Physics* 36: 2650.
15. Verellen D, De Ridder M, Tournel K, Duchateau M, Reynders T, et al. (2008) An overview of volumetric imaging technologies and their quality assurance for IGRT. *Acta Oncol* 47: 1271-1278.
16. Boda-Heggemann J, Walter C, Rahn A, Wertz H, Loeb I, et al. (2006) Repositioning accuracy of two different mask systems-3D revisited: comparison using true 3D/3D matching with cone-beam CT. *Int J Radiat Oncol Biol Phys* 66: 1568-1575.
17. Ma J, Chang Z, Wang Z, Wu QJ, Kirkpatrick JP, et al. (2009) ExacTrac X-ray 6 degree-of-freedom image-guidance for intracranial non-invasive stereotactic radiotherapy: comparison with kilo-voltage cone-beam CT. *Radiother Oncol* 93: 602-608.
18. Masi L, Casamassima F, Polli C, Menichelli C, Bonucci I, et al. (2008) Cone beam CT image guidance for intracranial stereotactic treatments: comparison with a frame guided set-up. *Int J Radiat Oncol Biol Phys* 71: 926-933.
19. Guckenberger M, Baier K, Guenther I, Richter A, Wilbert J, et al. (2007) Reliability of the bony anatomy in image-guided stereotactic radiotherapy of brain metastases. *Int J Radiat Oncol Biol Phys* 69: 294-301.
20. Baumert BG, Egli P, Studer S, Dehing C, Davis JB (2005) Repositioning accuracy of fractionated stereotactic irradiation: assessment of isocentre alignment for different dental fixations by using sequential CT scanning. *Radiother Oncol* 74: 61-66.
21. Chang Z, Wang Z, Ma J, O'Daniel JC, Kirkpatrick JP, et al. (2010) 6D image guidance for spinal non-invasive stereotactic body radiation therapy: Comparison between ExacTrac X-ray 6D with kilo-voltage cone-beam CT. *Radiother Oncol* 95: 116-121.